A Stochastic Numerical Analysis of Groundwater Fluctuations in Hillside Slopes for Assessing Risk of Landslides

山沙汰 危險度 推定을 위한 地下水位 變動의 推計論的 數値 解析

Lee, In-Mo*
李 寅 模

要 旨

본 논문에서는 무한사면에서 강우에 따른 지하수위 변동을 합리적으로 추정할 수 있는 추계론적 수치해석모델이 개발되었다. 특히, 투수계수, 비산출율(Specific Yield) 등의 지하수흐름에 필요한 계수들과 지하암반층의 공간적 변화에 의하여 지하수위가 공간적으로 변하는 효과에 관해 중점적으로 연구하였으며, 이러한 계수들의 공간적 변화를 추정하기 위하여 Kriging 이론을 도입하였다. Kriging 이론은 몇개의 제한된 실측치로부터 실측을 하지 못한 각각의 수치해석 요소에 불편, 최소분산을 갖는 값들을 추정할 수 있는 방법이다. 사면방향의 일차원 수치해석 모델, Kriging 이론, 1차근사해법을 조합하여 추계론적 1차원 수치해석 프로그램을 개발하였다. 또한 사면방향의 지하수위 변동뿐만 아니라, 횡방향의 변동도 조사하기 위하여 확정론적 2차원 모델도 개발하였다. 한 무한사면에 대하여 개발된 모델을 이용하여 예제해석을 한 결과 투수계수나 비산출율의 공간적 변화뿐만 아니라 지하암반층의 공간에 따른 요철도 지하수위의 공간적 변화에 큰 영향을 미침을 알게 되었다. 또한 지하수위는 사면방향으로 큰 변동을 보일뿐 아니라 횡방향으로의 변동 또한 무시할 수 없을 정도로 큼을 알 수 있었다. 개발된 모델의 결과들은 지하수위 변동에 의한 산사태 위험도 분석시에 이용될 수 있다.

Abstract

A stochastic numerical analysis for predicting the groundwater fluctuations in hillside slopes is performed in this paper to account for the uncertainties associated with the rainfall and site characteristics. The effect of spatial variabilities of aquifer parameters and the effect of temporal variability of recharge on the groundwater fluctuations are studied in depth. The Kriging is used to account for the spatial variabilities of aquifer parameters. This technique provides the best linear unbiased estimator of a parameter and its minimum variance from a limited number of measured data. A stochastic one-dimensional numerical model is developed by combining the groundwater flow model, the Kriging, and the first-order second-moment analysis. In addition, a two dimensional deterministic groundwater model is developed to study the change of ground-

* 正會員, 韓國科學技術院, 土木工學科 助敎授

water surface in the transverse direction as well as in the downslope direction. It is revealed that the undulations of the impervious bedrock in addition to the permeability and the specific yield have an important influence on the fluctuations of the groundwater surface. It is also found that the groundwater changes significantly in the transverse direction as well as in the downslope direction. The results obtained in this analysis may be used for evaluation of landslide risks due to high porewater pressure.

1. Introduction

Landslides on steep hillside slopes are common in mountainous parts around the world. They could cause loss of life, and destruction to natural environment, man-made structures, etc.[11,13,14,15] A common type of landslides is the debris flow or debris avalanche, where the shallow soil cover on a sloping bedrock becomes saturated and flows down the slope. Current methods of stability analysis in hillside slopes are based on the effective stress principle with an infinite slope. The safety factor F_s in Fig. 1 can be expressed as

$$F_s=\frac{\left[c'+\left\{(W_s+W_t)\frac{\cos\alpha}{l}-u\right\}*\tan\phi+S_r\right]*l}{(W_s+W_t)*\sin\alpha+F_w} \tag{1}$$

where W_s=the weight of soil, W_t=the weight of trees, F_w=the wind force on the trees, c' and ϕ'=the cohesion and angle of internal friction in terms of effective stresses, respectively, S_r=the contribution of the roots of trees to shear strength, and u=the porewater pressure. The porewater pressure, u, is related to the fluctuation of the groundwater surface and can be obtained from (See Fig. 1)

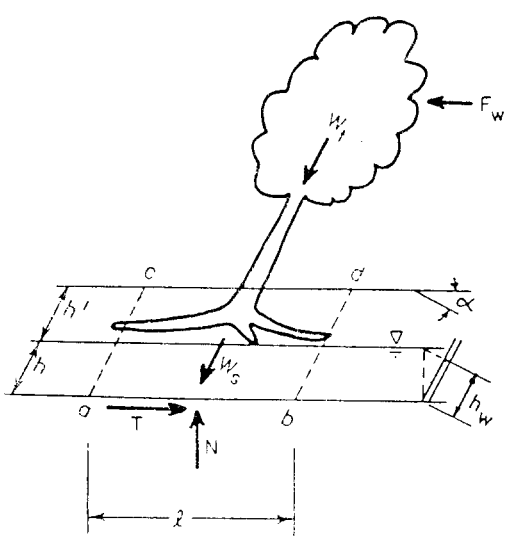

Fig. 1. Forces on Sliding Soil Mass

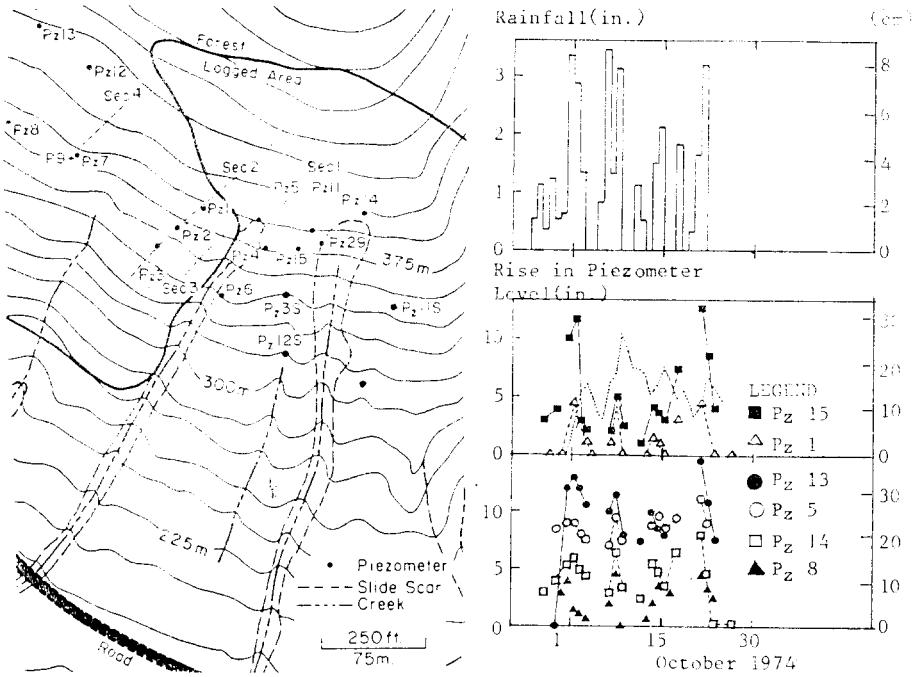

(a) Locations of Piezometers (b) Levels of Piezometers

Fig. 2. Piezometric Levels, 1974, Maybeso Valley of Alaska

$$u=\gamma_w h_w=\gamma_w h\cos^2\alpha \tag{2}$$

where γ_w is the unit weight of water. Thus, the movement of groundwater is one of the important factors initiating landslides. In other words, landslide risk may be expressed as the probability of the porewater pressure exceeding the value required to produce shear failure. The groundwater fluctuates significantly with a function of space as well as with a function of time, associated with rainfall.[10,13,14] A typical example which shows the fluctuations is shown in Fig. 2.[13,14] As shown in Fig. 2, the rise in piezometer changes significantly from point to point at a given time, besides it shows significant changes with respect to time associated with rainfall intensity. This paper addresses the fluctuations of the groundwater surface due to infiltration of rainfall and drainage by gravity flow. A stochastic numerical analysis is formulated to account for the uncertainties associated with rainfall and site characteristics.

2. Theoretical Basis of Groundwater Flow

For the groundwater flow in a shallow soil cover on a sloping impervious bedrock, the following simplifying assumptions are used:

1) Only saturated flow is considered. This means that the flow in the unsaturated zone above water surface is replaced by vertical flow conveying recharge from the ground surface down

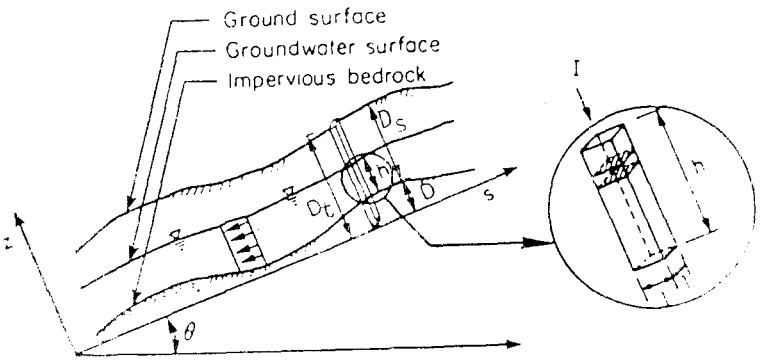

Fig. 3. Groundwater Flow on a Sloping Bed

to the water surface.

2) The streamlines in the s-direction are parallel to the s-axis (see Fig. 3) and the total head at a point in the s-direction is same along the z-axis. It is called the extended Dupuit-Forchheimer assumption.[1,3,6]

3) The flow occurs mainly in the downslope direction along the s-axis. This assumption leads to a one-dimensional idealization.

Considering a thin soil cover overlying impervious bedrock on a hillslope of slope angle θ (see Fig. 3), the flow quantity within the saturated zone is

$$Q=\left(-K*\frac{\partial \Phi}{\partial s}\right)*(1*h) \tag{3}$$

in which Φ=total hydraulic head, K=permeability of soil, h=depth of the groundwater surface above the impervious bedrock, measured perpendicular to the s-axis. The total head, Φ, is a combination of the elevation head and the porewater pressure head:

$$\Phi=s*\sin\theta+(h+D)*\cos\theta \tag{4}$$

It has been common to assume that D in Fig. 3 is zero in the governing equation. This assumption is reasonable if h in Fig. 3 is much greater than D. However, for the shallow soil cover on the bedrock, groundwater fluctuations may be sensitive to the topography of bedrock, and it may not be ignored in the equation. D can be expressed as

$$D=D_t-D_s \tag{5}$$

in which D_t=depth between the ground surface and the s-axis and D_s=depth of the soil cover. The continuity equation is

$$S_y*\frac{\partial h}{\partial t}=I-\frac{\partial Q}{\partial s} \tag{6}$$

in which S_y=specific yield, I=input per unit area parallel to the s-axis. Eqs. 3 to 6 are combined to give

$$S_y*\frac{\partial h}{\partial t}=R*\cos\theta+\frac{\partial}{\partial s}\left[K*h*\left\{\cos\theta*\left(\frac{\partial h}{\partial s}+\frac{\partial D_t}{\partial s}-\frac{\partial D_s}{\partial s}\right)+\sin\theta\right\}\right] \tag{7}$$

in which $R=I/\cos\theta$. Since Eq. 7 can not be solved analytically, a numerical technique is used.[2] The finite difference form of Eq. 7 is

$$h_i^{t+\Delta t}=h_i^t+\frac{\Delta t}{S_{yi}}* \tag{8}$$

$$*\frac{1}{\Delta s}\left[\left(\frac{K_{i+1}+K_i}{2}\right)\left(\frac{h_{i+1}+h_i}{2}\right)\left\{\frac{\cos\theta}{\Delta s}(h_{i+1}-h_i+D_{ti+1}-D_{ti}-D_{si+1}+D_{si}+\sin\theta\right\}$$
$$-\left(\frac{K_i+K_{i-1}}{2}\right)\left(\frac{h_i+h_{i-1}}{2}\right)\left\{\frac{\cos\theta}{\Delta s}(h_i-h_{i-1}+D_{ti}-D_{ti-1}-D_{si}+D_{si-1})+\sin\theta\right\}\Big]^t$$
$$+R_i^t*\cos\theta$$

with space index i, and time index t.

3. A Stochastic Model for Groundwater Flow

3.1. First-order Seond-moment Analysis

The numerical flow model, Kriging, and first-order second-moment analysis are combined to develop a stochastic model for the prediction of the depth of the groundwater surface in a shallow soil cover overlying the impervious bedrock. The first-order second-moment analysis is characterized by the following two features:

1) Under the assumption of statistical homogeneity for the medium, the random vector x is characterized by the first two moments. That is, the state vector is described in terms of its mean vector and covariance matrix:

$$x(t)=[\bar{x}(t), C_{x(t)}] \tag{9}$$

in which $\bar{x}(t)$=mean of the random vector $x(t)$, and $C_{x(t)}$=its covariance matrix.

2) Only the first order terms in the Taylor's expansion are used in dealing with functional relationships among random variables. In other words, if the function is expressed as

$$h(t+\Delta t)=f[h(t),\ u(t),\ K] \tag{10}$$

in which $h(t+\Delta t)$ and $h(t)$=state vectors at time $t+\Delta t$ and t, respctively, $u(t)$=vector of the inputs to the system, and K=vectors of the parameters of the model, then the furction can be linearized as

$$h(t+\Delta t)=f[\bar{h}(t),\bar{u}(t),\bar{K}]+\frac{\partial f}{\partial h(t)}[h(t)-\bar{h}(t)]+\frac{\partial f}{\partial u(t)}[u(t)-\bar{u}(t)]+\frac{\partial f}{\partial K}[K-\bar{K}] \tag{11}$$

It is assumed that the K, the S_y, the D_s, and the R are random variables. The aquifer parameters between two elements are correlated with each other, and can be expressed as

$$K=[\bar{K},\ C_K] \tag{12a}$$
$$S_y=[\bar{S}_y,\ C_{S_y}] \tag{12b}$$
$$D_s=[\bar{D}_s,\ C_{D_s}] \tag{12c}$$

in which $(\bar{\cdot})$=state vector of mean values for each element, and $C_{(\cdot)}$=covariance matrix. Among these aquifer parameters, the permeability and the specific yield are correlated and the cross-covariance matrix between these two is represented as C_{KS_y}.

The formulation developed by Dettinger and Wilson[5,12] is adoptd to derive the equations for the first-order second-moment analysis. Assume an augmented state vector

$$X_{(t)}=\begin{bmatrix} h \\ K \\ S_y \\ D_s \\ R_{(t)} \end{bmatrix} \tag{13}$$

with the covariance matrix

$$C_{X(t)}=\begin{bmatrix} C_{h(t)} & C_{hK(t)} & C_{hS_y(t)} & C_{hD_s(t)} & C_{hR(t)} \\ C^T_{hK(t)} & C_K & C_{KS_y} & — & — \\ C^T_{hS_y(t)} & C^T_{KS_y} & C_{S_y} & — & — \\ C^T_{hD_s(t)} & — & — & C_{D_s} & — \\ C^T_{hR(t)} & — & — & — & C_{R(t)} \end{bmatrix} \tag{14}$$

in which superscript T represents transpose of the matrix. The covariance matrix of the predictive model is

$$C_{X(t+\Delta t)}=\begin{bmatrix} C_{h(t+\Delta t)} & C_{hK(t+\Delta t)} & C_{hS_y(t+\Delta t)} & C_{hD_s(t+\Delta t)} & C_{hR(t+\Delta t)} \\ C^T_{hK(t+\Delta t)} & C_K & C_{KS_y} & — & — \\ C_{hS_y(t+\Delta t)} & C^T_{KS_y} & C_{S_y} & — & — \\ C^T_{hD_s(t+\Delta t)} & — & — & C_{D_s} & — \\ C^T_{hR(t+\Delta t)} & — & — & — & C_{R(t+\Delta t)} \end{bmatrix} \tag{15}$$

$$=\begin{bmatrix} Q & P & E & N & F \\ — & I & — & — & — \\ — & — & I & — & — \\ — & — & — & I & — \\ — & — & — & — & I \end{bmatrix} C_{X(t)} \begin{bmatrix} Q^T & — & — & — & — \\ P^T & I & — & — & — \\ E^T & — & I & — & — \\ N^T & — & — & I & — \\ F^T & — & — & — & I \end{bmatrix}$$

in which Q, P, E, N, and F are sensitivity matrices. Manipulating this matrix multiflication leads to the following covariance matrices:

$$\begin{aligned} C_{h(t+\Delta t)}=&Q\ C_{h(t)}Q^T+Q\ C_{hK(t)}P^T+P\ C^T_{hK(t)}Q^T+Q\ C_{hS_y(t)}E^T \\ &+E\ C^T_{hS_y(t)}Q^T+Q\ C_{hD_s(t)}N^T+N\ C^T_{hD_s(t)}Q^T+Q\ C_{hR(t)}F^T \\ &+F\ C^T_{hR(t)}Q^T+F\ C_{R(t)}F^T+P\ C_KP^T+E\ C_{S_y}E^T \\ &+P\ C_{KS_y}E^T+E\ C^T_{KS_y}P^T+N\ C_{D_s}N^T \end{aligned} \tag{16a}$$

$$C_{hK(t+\Delta t)}=Q\ C_{hK(t)}+P\ C_K+E\ C_{KS_y} \tag{16b}$$

$$C_{hS_y(t+\Delta t)}=Q\ C_{hS_y(t)}+P\ C_{KS_y}+EC_{S_y} \tag{16c}$$

$$C_{hD_s(t+\Delta t)}=Q\ C_{hD_s(t)}+N\ C_{D_s} \tag{16d}$$

$$C_{hR(t+\Delta t)}=Q\ C_{hR(t)}+F\ C_{R(t)} \tag{16e}$$

Referring to these equations, the uncertainty of the predicted groundwater surface at time $t+\Delta t$ is the function of uncertainties of the $h(t)$, uncertainties of the K, the S_y and the D_s, uncertainty of the recharge, $R(t)$, and cross-correlations.

3.2 Kriging

The permeability (K), the specific yield (S_y), and the depth of soil cover overlying impervious bedrock (D_s) change from point to point along a slope. This inherent spatial variability can be eliminated if we can determine exact values of these at every point within the domain and take these into consideration in the analysis. However, it is not easy to get measured values for every element. Only limited number of measured data are usually obtained from tests. The method of Kriging is used to estimate the parameters for every element in the finite difference mesh. The Kriging is an estimation technique which provides the best linear unbiased estimator of parameters for each element.[4,8]

Consider an element V having a true unknown spatially averaged value Z_V, and a series of n samples of measured values Z_i ($i=1,\ldots,n$). The best estimater of Z_V, Z^*, can be expressed as

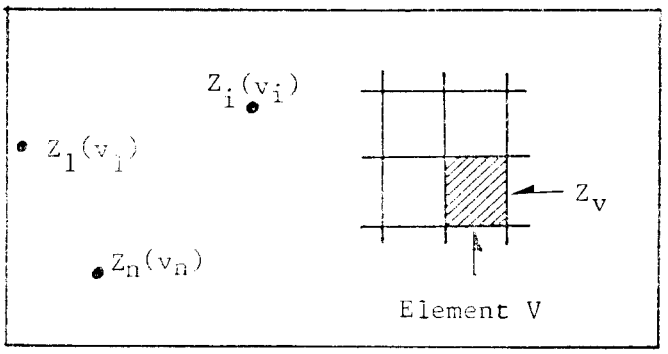

Fig. 4. Kriging

a linear combination of n data values (see Fig. 4) as

$$Z^*=\sum_{i=1}^{n} a_i * Z_i \tag{17}$$

The weights a_i should be calculated so as to ensure that the estimator is unbiased and that the estimation variance is minimal. The non-bias condition is satisfied by

$$\sum_{i=1}^{n} a_i - 1 = 0 \tag{18}$$

If $E(Z)=m$, the estimation variance may be written in terms of the covariance as

$$\begin{aligned} VAR(Z^*) &= E(Z_v - Z^*)^2 \\ &= COV(V,V) - 2*\sum_i a_i * COV(V,\ v_i) + \sum_i \sum_j a_i * a_j * COV(v_i, v_j) \end{aligned} \tag{19}$$

where $COV(V,V)$=the variance of spatially averaged parameter over element V, $COV(V,v_i)$= the covariance of element V and sample v_i, $COV\ (v_i,v_j)$=the covariance of measured sample v_i and v_j. The weights a_i that minimize this error variance are found by the association of a Lagrange multiplier, 2μ, with the constraint given in Eq. 18, and by the solution of the first order conditions directly for a_i and μ as given below. The Lagrangian is

$$L(a,\ \mu) = COV(V,V) - 2*\sum_j a_i * COV(V,\ v_i) + \sum_i \sum_i a_i * a_j * COV(v_i,\ v_j) - 2*\mu(1 - \sum_i a_i) \tag{20}$$

The first-order necessary conditions are

$$\frac{\partial L}{\partial a_i} = 0 = -2*COV(V,\ v_i) + 2*\sum_j a_j * COV(v_i,\ v_j) - 2*\mu \tag{21}$$

and

$$\frac{\partial L}{\partial \mu} = 0 = \sum_i a_i - 1 \qquad i = 1, 2, \cdots, n \tag{22}$$

If we express these in matrix form,

$$\begin{bmatrix} COV(v_1,\ v_1) & COV(v_1,\ v_2)\cdots COV(v_1,\ v_n) & -1 \\ \vdots & & \vdots \\ COV(v_i,\ v_j) & & -1 \\ \vdots & & \vdots \\ COV(v_n,\ v_1) & COV(v_n,\ v_2)\cdots COV(v_n,\ v_n) & -1 \\ 1 & 1 \quad \cdots \quad 1 & 0 \end{bmatrix} \begin{bmatrix} a_1 \\ \vdots \\ a_i \\ \vdots \\ a_n \\ \mu \end{bmatrix} = \begin{bmatrix} COV(V,\ v_1) \\ \vdots \\ COV(V,\ v_i) \\ \vdots \\ COV(V,\ v_n) \\ 1 \end{bmatrix} \tag{23}$$

or

$$[K_{VV}] * [a] = [K_{Vv}] \tag{24}$$

Since K matrices have fully known elements, we can express Eq. 24 as

$$[a] = [K_{VV}]^{-1} * [K_{Vv}] \tag{25}$$

Therefore, estimates of the parameters become

$$Z^*=\sum_{i=1}^{n} a_i * Z_i \tag{26}$$

where a_i can be obtained by using Eq. 25, and

$$VAR(Z^*)=COV(V,\ V)-[a]^T*[K_{V\cdot}] \tag{27}$$

Eqs. 25, 26, and 27 are used for the best estimation of parameters such as the K, the S_y, and the D_s for each element.

3.3 Recharge Model

For estimating the recharge from rainfall, the model developed by Johnson and Sangrey et al. is used in this study.[7,10] The recharge, R, can be expressed as

$$R=P-Q_R-E \tag{28}$$

in which P=precipitation, Q_R=runoff, and E=evapotranspiration. Because both the runoff and the evapotranspiration are functions of the precipitation, the recharge, R, is also a function of the precipitation. That is:

$$Q_R=f(P) \tag{29}$$

$$E=f(P) \tag{30}$$

and

$$R=f(P) \tag{31}$$

Further, Goldschmidt suggested linear functions between the precipitation and the runoff and the evapotranspiration:

$$Q_R=c_0+c_1*P \tag{32}$$

$$E=d_0+d_1*P \tag{33}$$

Then, the recharge, R, can be expressed as

$$R=(-c_0-d_0)+(1-c_1-d_1)*p \tag{34}$$

On the other hand, Thornthwaite proposed a model which could predict the monthly potential evapotranspiration, PE_m, by expressing it in terms of the monthly temperature. T_m:

$$PE_m=f(T_m) \tag{35}$$

The potential evapotranspiration is the upper bound of the evapotranspiration. Therefore, it usually overstimates the actual monthly evapotranspiration. To overcome this problem Johnson proposed a model which combined Goldschmidt method with Thornthwaite's. To apply his model, the annual evapotranspiration should be observed. It can be expressed as

$$E_y=d_0+d_1*P_y \tag{36}$$

in which E_y=annual evapotranspiration, and P_y=annual precipitation. The coefficients d_0, and d_1 are obtained from the regression analysis between E_y and P_y. His model is expressed as:

$$R_m=d_{0m}+d_{1m}*P_m \tag{37}$$

in which R_m=mean monthly recharge, and P_m=mean monthly precipitation, $d_{0m}=-d_0*(PE_m/PE_y)$, and $d_{1m}=1-d_1*(PE_m/PE_y)*(P_y/P_m)$. To obtain the recharge on a daily basis instead of a month, Eq. 37 has to be divided into the number of days a month, n_d. That is:

$$R_d=d_{0m}/_{nd}+d_{1m}*(P_m/_{nd})=d_{0m}/_{nd}+d_{1m}*P_d \tag{38}$$

The drawback of using Eq. 38 for the estimation of daily recharge is that change of the daily recharge from a month to the next is abrupt due to change in the coefficients (d_{0m} and d_{1m})

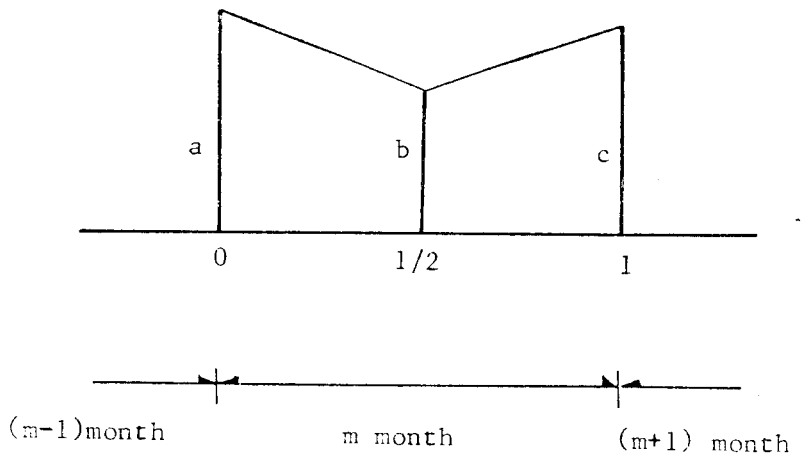

$$a = \frac{1}{2}(d_{m-1} + d_m)$$

$$b = \frac{1}{4}(-d_{m-1} + 6d_m - d_{m+1})$$

$$c = \frac{1}{2}(d_m + d_{m+1})$$

Fig. 5. Linear Spline Method

between elements. To overcome this problem, the linear spline method was developed by Johnson to make these coefficients vary smoothly rather than adrupt. For the coefficients, d_{0m} and d_{1m}, two straight lines within a month instead of constants are used. One line is used between at the beginning of a month and at the center, and the other is used for the second half parts of a month. These are shown in Fig. 5.

4. A Two-Dimensional Groundwater Model

The one-dimensional groundwater model is based on the assumption that the flow occurs mainly in the downslope direction. This assumption implies that the bedrock profile is approximately horizontal in the transverse direction. As a matter of fact, it is not true in most cases. Slopes in the transverse direction concentrate groundwater flow in the depressed zones such that the depth of the groundwater surface is larger in these zones than in surrounding areas.[9,11] Due to this reason, more landslides occur in the depressed zones than in others. To study the change of the groundwater surface in the transverse direction as well as in the downslope direction, a two-dimensional groundwater model is also developed. Since the main purpose of this model is to study the spatial variation of the groundwater surface in the transverse direction or to study the effect of the transverse flow on the depth of the groundwater surface in the depressed zones, only deterministic approach based on mean properties is considered. The direction of the transverse flow in the zone '*R*' is opposite to that in the zone '*L*' shown in Fig. 6. Therefore, two zones have to be solved separately.

The following assumptions are used in the two-dimensional analysis:

1) As in the one-dimensional analysis, only saturated flow is considered.
2) In the downslope direction, the streamlines are parallel to the s-axis (see Fig. 6).
3) For the flow in the transverse direction, the Dupuit-Forchheimer assumption is used, which assumes that the flow lines within the saturated zone are horizontal, The reason is as follows. 'First', the slope angle in the transverse direction is usually small compared to that in the downslope direction. Second, this assumption is at least correct in the depression boundary(see Fig. 6).

Consider a thin soil cover overlying impervious bedrock on a hillslope of angle θ in the downslope direction and angle α in the transverse direction (see Fig. 7). The flow within the saturated zone can be described by Darcy's law:

$$V_x = -K_x * \frac{\partial \Phi}{\partial x} \tag{39a}$$

$$V_s = -K_s * \frac{\partial \Phi}{\partial s} \tag{39b}$$

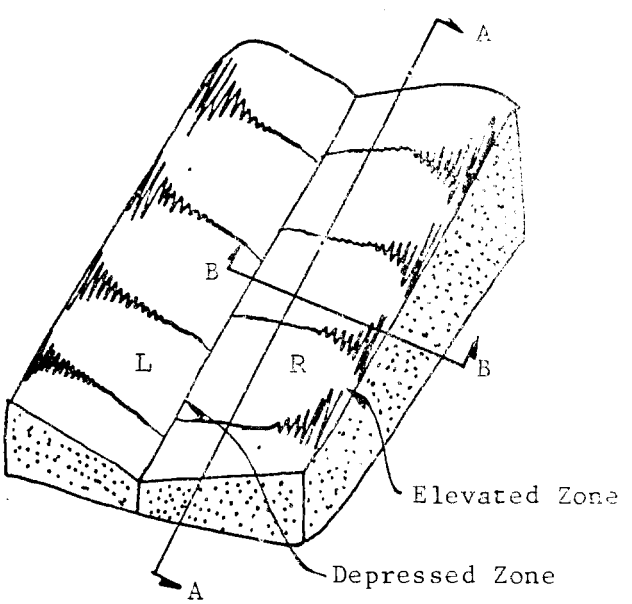

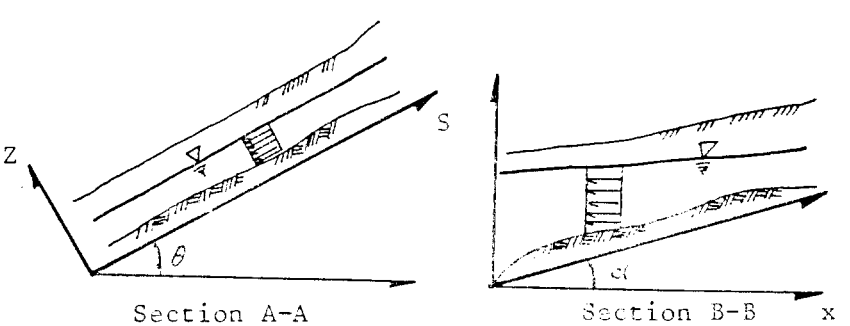

Fig. 6. Two-Dimensional Groundwater Flow on a Sloping Bed

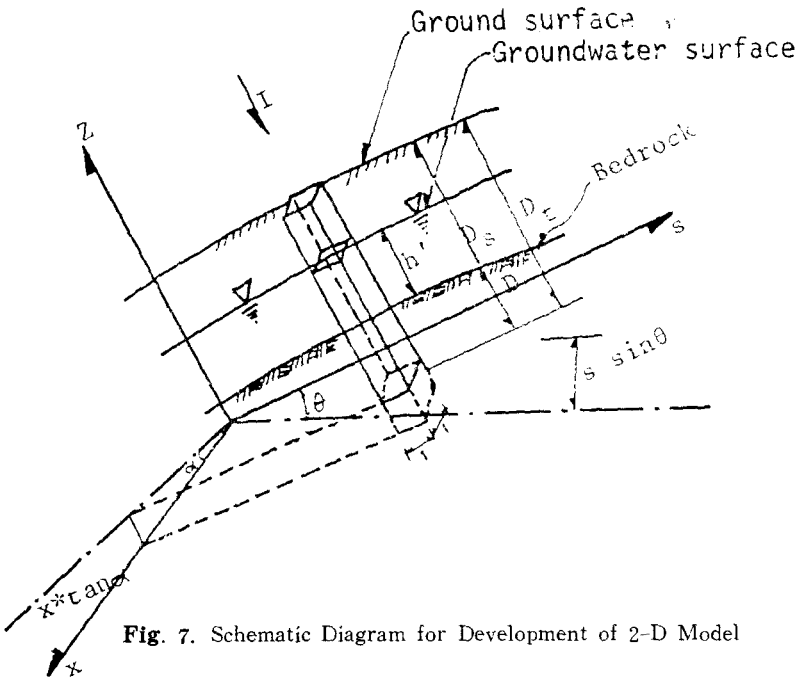

Fig. 7. Schematic Diagram for Development of 2-D Model

in which Φ is the total potential head which is the combination of the pressure head and the elevation head. That is:

$$\Phi=(h+D)*\cos\theta+s*\sin\theta+x*\tan\alpha \tag{40}$$

From the continuity of the groundwater flow, and by assuming the permeability to be isotropic, the following two-demensional equation is obtained:

$$S_y*\frac{\partial h}{\partial t}=R*\cos\theta+\frac{\partial}{\partial x}\left[K*h*\left\{\cos\theta*\left(\frac{\partial h}{\partial x}+\frac{\partial D_t}{\partial x}-\frac{\partial D_s}{\partial x}\right)+\tan\alpha\right\}\right]$$
$$+\frac{\partial}{\partial s}\left[K*h*\left\{\cos\theta*\left(\frac{\partial h}{\partial s}+\frac{\partial D_t}{\partial s}-\frac{\partial D_s}{\partial s}\right)+\sin\theta\right\}\right] \tag{41}$$

As in the one-dimensional case, the explicit numerical technique is used. For the estimation of aquifere parameters for each element, the two-dimensional Kriging has to be used.

5. Illustrative Examples

The method developed is used to compute the groundwater fluctuations in a hypothetical slope, that represents a small drainage basin shown in Fig. 8a. The slope and the finite difference meshes for the one-dimensional analysis are shown in Fig. 8d. The values of K, S_y, and D_s are assumed to be observed at specific points. The location of these points and the measured values are shown in Figs. 8b and c. The recharage is shown in Fig. 9a. The computed mean and coefficient of variation (C.O.V.) of h along the slope are shown in Fig. 10a and b. The h's show relatively highy values in the area of low permeability when compared to those in the area of high permeability. The computed mean and coefficient of h as a function of time are shown in Fig. 9b and c, respectively for two elements. The rise and drop of h as a function of time near the head of valley is more abrupt than that near the mouth of valley.

The effect of bedrock topography on h is also studied by comparing h's with a smooth topog-

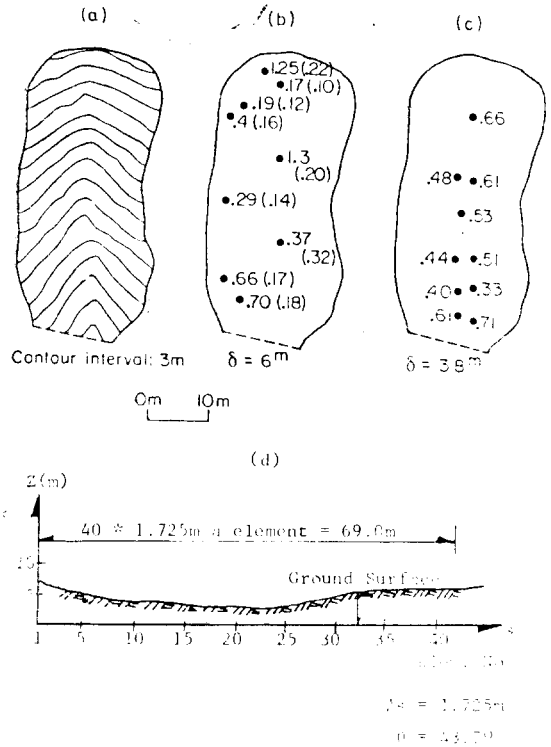

(a) Topographic Map,
(b) Permeability, m/day, and Specific Yield in ( ),
(c) Soil Thickness, m.,
(d) Finite Difference Meshes

Fig. 8. Hypothetical Slope

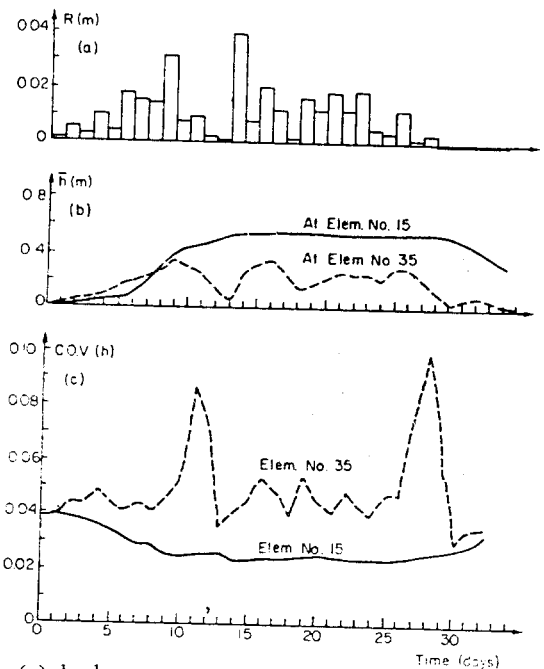

(a) hecharge,
(b) Mean of h,
(c) Coefficient of Variation (C.O.V.) of h

Fig. 9. Groundwater Fluctuations as Function of Time,

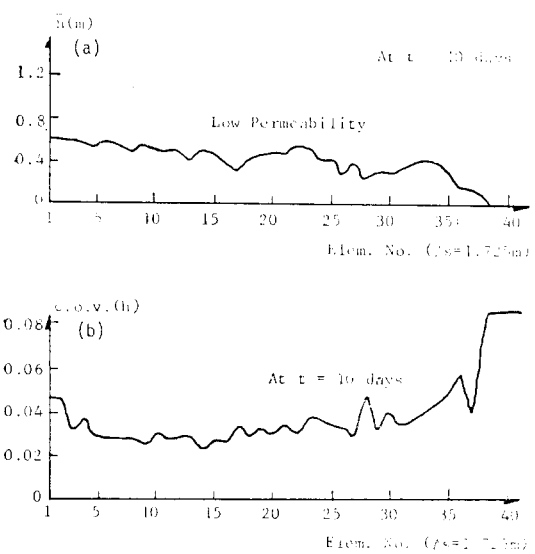

(a) Mean of h,
(b) Coefficient of Variation (C.O.V.) of h

Fig. 10. Groundwater Fluctuations as Function of Space

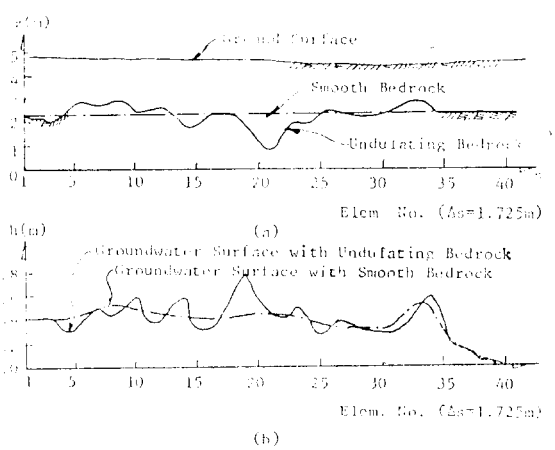

(a) Bedrock Topography,
(b) Profiles of Groundwater Fluctuations

Fig. 11. Effect of Bedrock Topography

raphy and with an undulating topography shown in Fig. 11a. The typical results are shown in Fig. 11b. The results show that the influence of the bedrock topography is an important factor.

The same basin shown in Fig. 8a is used to illustrate the deterministic two-dimensional analysis developed in this paper. Finite difference meshe are shown in Fig. 12. All input data are same as those for the one-dimensional case. A typical profile of the mean groundwater surface in the transverse direction is shown in Fig. 13. The variation of the mean groundwater surface from the depressed zone to the elevated zone is significant. It ranges from full saturation to zero waterhead. It is also observed that full saturation is quickly developed in most depressed zones except at few upstream parts.

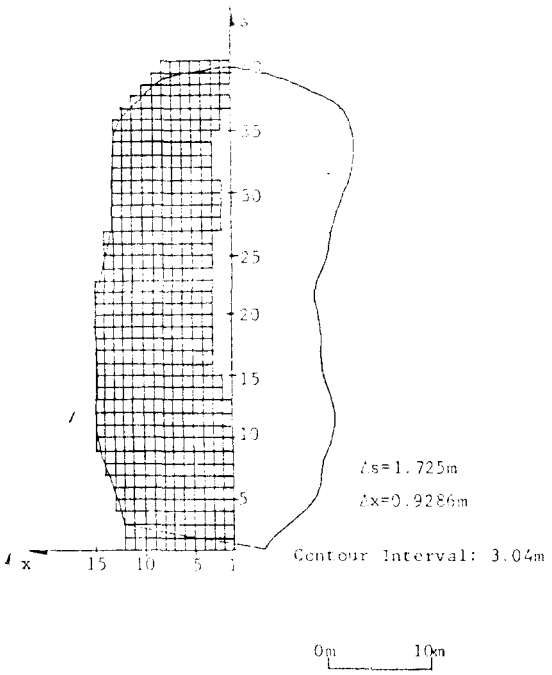

Fig. 12. Two-Dimensional Finite Difference Meshes

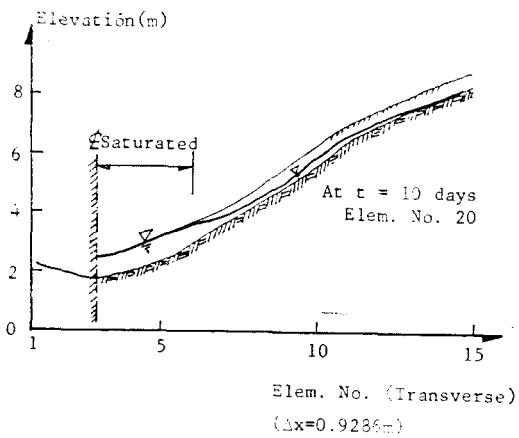

Fig. 13. Profiles of Groundwater Surface in Transverse Direction.

6. Summary and Conclusions

A stochastic numerical model for the prediction of the groundwater fluctuations in a shallow soil cover on a sloping bedrock is developed. Groundwater fluctuations are found to be significant as a function of space as well as a function of time. It is also revealed that in addition to the permeability and the specific yield, the undulations of the impervious surface have an important influence on the groundwater fluctions.

A two-dimensional groundwater model besides the one-dimensional stochastic model is also developed to study the change of the groundwater surface in the transverse direction as well as in the downslope direction. It is revealed that the groundwater changes significantly in the transverse direction from zero waterhead in the elevated zones to full saturation in the depressed zones.

The approach obtained in this analysis may be used in the reliability analysis for assessing the risk of landslides in hillside slopes. The approach formulated in this paper is general in nature and can also be used in cases where there is a change in slope, nonstationary processes, or heterogeneous soil deposits with some modifications.

References

1. Beven, K., "Kinematic Subsurface Stormflow", Water Resour, Res., Vol. 15, 1981, pp. 1419~1424.
2. Carnahan, B., Luther, H.A., and Wilkes, J.O., Applied Numerical Methods, John Wiley, 1969.
3. Childs, E.C., "Drainage of Groundwater Resting on a Sloping Bed", Water Resour. Res., Vol. 7, No. 5, 1971, pp. 1256~1263.
4. David, M., Geostatistical Ore Reserve Estimation (Developments in Geomathematics, Vol. 2), Elsevier, Amsterdam, 1977.
5. Dettinger, M.D., and Wilson, J.L., "First Order Analysis of Uncertainty in Numerical Models of Groundwater Flow, Part 1. Mathematical Development", Water Resour. Res., Vol. 17, No. 1, 1981, pp. 149~161.
6. Henderson, F.M., and Wooding, R.A., "Overland Flow and Groundwater Flow from a Steady Rainfall of Finite Duration", J. of Geophys. Res., Vol. 69, 1964, pp. 1531~1540.
7. Johnson, K.H., "A Predictive Method for Groundwater Levels", M.S. Thesis, Cornell University, Ithaca, N.Y., 1977.
8. Journel, A.G., and Huijbregts, Ch. J., Mining Geostatistics, Academic Press, London, 1978.
9. Pierson, T.C., Factors Controlling Debris-Flow Initiation on Forested Hillslope in the Oregon Cost Range, Ph. D. Dissertation, University of Washington, Seattle, 1977.
10. Sangrey, D.A., Harrop-Williams, K.O., and Klaiber, J.A., "Predicting Groundwater Response to Precipitation", J. of Geotechnical Engineering Division, ASCE, Vol. 110, No. 7, 1984, pp. 957~975.
11. Sidle, R.C., "Shallow Groundwater Fluctuations in Unstable Hillslopes of Coastal Alaska", Zeitschrift für Gletscherkunde und Glazialgeologie, Vol. 20, No. 2, 1985, Forestry Science Lab., Pacific Northwest Forest and Range Experiment Station, U.S. Dept. of Agriculture, Forest Service, Juneau.
12. Wilson, J., Kitanidis, P., and Dettinger, M., "State and Parameter Estimation in Groundwater Models: Applications of Kalman Filter to Hydrology", Hydraulics and Water Resources, edited by C.L. Chiu, University of Pittsburgh, Pittsburgh, 1978, pp. 657~679.
13. Wu, T.H., Mckinnell III, W.P., and Swanston, D.N., "Strength of Tree Roots and Landslides on Prince of Wales Island, Alaska", Canadian Geotechnical J., Vol. 16, 1979, pp. 19~33.
14. Wu. T.H., and Swanston, D.H., "Risk of Landslides in Shallow Soils and Its Relation to Clearcutting in Southeastern Alaska", Forest Science, Vol. 26, No. 3, 1980, pp. 495~510.
15. Zaruba, Q., and Mencl, V. (1969), Landslides and Their Control, Elsevier, Amsterdam, 1969.

(접수일자 1987. 10. 15)